Observations of the Mean and Turbulence Structure of the Marine Boundary Layer over the Bay of Bengal during MONEX 79

TEDDY HOLT AND SETHU RAMAN

Department of Marine, Earth and Atmospheric Sciences, North Carolina State University, Raleigh, NC 27695

ABSTRACT

Radiosondes from Soviet ships along with dropsondes and mean and turbulence data from the National Center for Atmospheric Research (NCAR) Electra gust probe aircraft are analyzed to infer the structure of the monsoon marine boundary layer during MONEX 79. Results of mean wind profiles indicate the existence of a jetlike structure in the upper part of the boundary layer during the more suppressed "monsoon-break" conditions. The thermal structure of the monsoon boundary layer during these break conditions is characterized by near-neutral to slightly unstable conditions. There was an approximate balance of forces in the monsoon boundary layer between advective acceleration, friction and geostrophic departure. Advective acceleration was found to be a significant term, especially in the lower levels of the boundary layer. This contrasts with typical trade-wind boundary layers in which acceleration is generally negligible.

Results indicate that turbulence statistics associated with wind speed components and temperature in the monsoon boundary layer during MONEX 79 are generally large. Profiles of momentum and virtual temperature flux change sign at altitudes as low as 30 to 50% of the boundary layer height. The turbulent kinetic energy budget indicates that buoyancy is not a dominant source term above, roughly, one-third the boundary layer height. Viscous energy dissipation and turbulent transport are the important sink terms in the lowest one-half of the boundary layer.

1. Introduction

Monsoon depressions that form over the Bay of Bengal during the Indian southwest monsoon cause precipitation over a wide area in northern India. Their generation at the head of the Bay of Bengal seems to depend on the location of the monsoon trough in relation to the Gangetic plains. When the trough is located along the Gangetic plains protruding into the Bay of Bengal, active monsoon conditions seem to prevail (Rao, 1976). When the trough migrates farther to the north and lies along the foothills of the Himalayas, it coincides with a break in the monsoon (Sikka, 1978). Boundary layer profiles at a Bay of Bengal coastal site (Digha) obtained from pilot balloon soundings for the period 14 July to 4 August 1979 during MONEX 79 indicate two distinct boundary layers. About 70% of the wind profiles showed the presence of a jetlike flow in the boundary layer. Figure 1 shows pilot balloon wind profiles from Digha indicating a jetlike feature on 16 July and no jet on 22 July. Examination of the synoptic surface weather chart for 16 July indicated the monsoon trough to be located far northward, similar to the weather map of 14 July (Fig. 2) near the foothills of the Himalayan Mountains when the jetlike structure was noticed in the wind profiles. This location of the trough is synonymous with the "break" in the monsoon when the depressions fail to form over the Bay of Bengal with consequent lack of

rain over a major part of India. About 30% of the wind profiles did not show any jetlike feature (Fig. 1) and the wind speed was nearly constant in the lower layers to a height of about 350 m. Such a wind structure occurred when the monsoon trough was aligned with the Gangetic plains and protruded over the head of the Bay of Bengal (Fig. 3). This positioning of the trough usually leads to an "active" monsoon period. Active monsoon conditions are usually periods of heavier rainfall while break conditions show a dramatic decrease in rainfall.

Thus, the interaction between the boundary layer and mesoscale and even synoptic scale motions is such that one would expect the marine boundary layer processes existing over the Bay of Bengal during the monsoon to play a significant role in cyclogenesis. The formation and structure of depressions have been investigated in the past (Kotteswaram and George, 1958; Krishnamurti et al., 1975; Krishnamurti and Bhalme, 1976). A study of the boundary layer processes had been difficult because of lack of data. The Monsoon Experiment (MONEX) 79 provided some boundary layer observations over the Bay of Bengal during July and August of 1979. Very little information is known about the structure of the marine boundary layer over the Bay of Bengal during the Indian southwest monsoon. However, the marine boundary layer processes over the trade wind tropical oceans have been studied by several investigators (Donelan and Miyake, 1973;
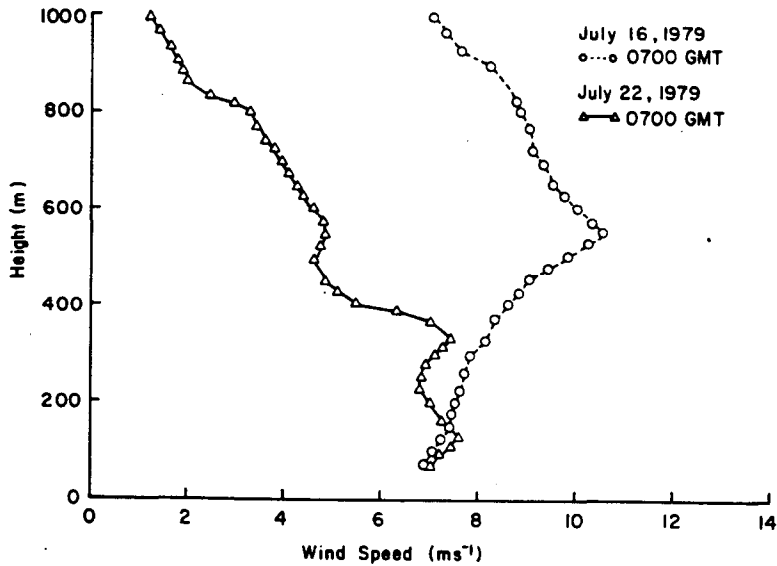
FIG. 1. Mean wind speed profiles obtained from Digha observations
for 16 July (break monsoon) and 22 July (active monsoon).

LeMone, 1980; Pennell and LeMone, 1974; Sommeria and LeMone, 1978).

The purpose of this paper is to present and discuss the results of the mean and turbulence structure of the

marine boundary layer over the Bay of Bengal using dropwindsonde and low-level flight data collected by the NCAR Electra aircraft, tower data at a coastal site (Digha) and observations from U.S.S.R. ships during MONEX 79.
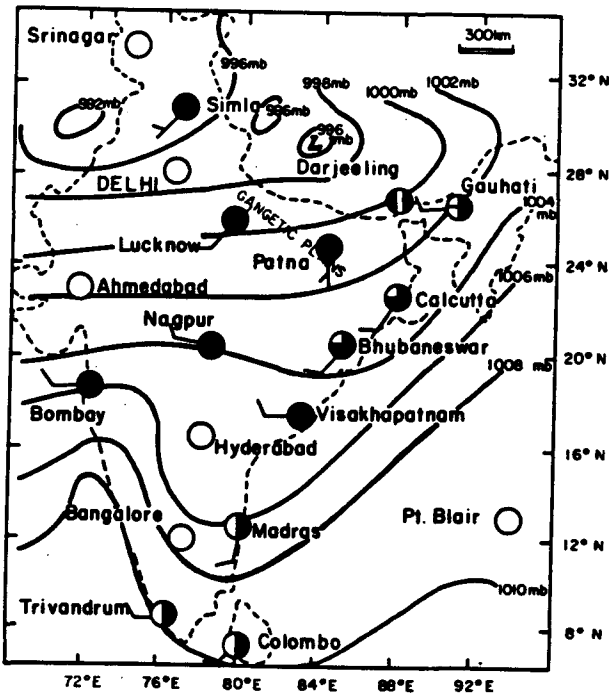

FIG. 2. Surface map for approximately 1200 GMT on 14 July 1979 obtained from hourly observations. Note the position of the monsoon trough roughly along 29°N latitude at the foothills of the Himalayas. Break conditions existed for this day. Wind barbs represent 10 kt with lack of barbs indicating missing data.
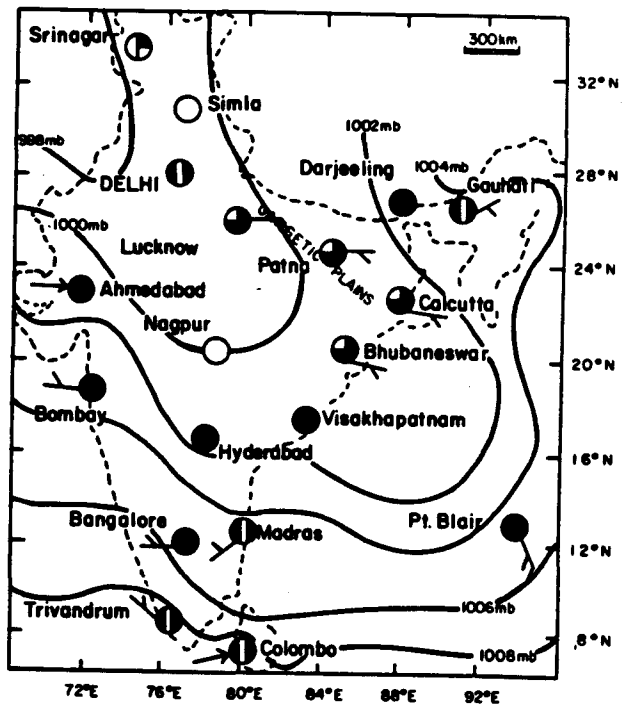

FIG. 3. Surface map for 0330 GMT on 29 July 1979 during active monsoon conditions. Note the position of the trough dipping into the Bay of Bengal.

2. Large scale flow: 1–31 July

The 1979 monsoon was late and was associated with prolonged weak and "break" monsoon periods. Rainfall was very much below normal with drought conditions in many areas. The period 1–11 July was characterized by the development and dissipation of one monsoon depression and the associated monsoon trough. The low-level monsoon trough developed on 2 July and by 4 July had dipped southeast over the Bay of Bengal. The first indications of the monsoon depression were evident on 4 July over the northeastern Bay of Bengal. The depression intensified and moved inland on 8 July. The depression had a large horizontal extent but the rainfall was significantly less than normal. By 10 July the depression had dissipated. Low-level westerlies began to reestablish over India by 11 July. The period 12 to 21 July was characterized by "break" monsoon conditions in which the monsoon trough was generally farther north along the foothills of the Himalayas with convective activity limited over India. The surface weather map for 14 July, obtained from hourly observations (Fig. 2), is typical of "break" conditions. Low-level westerly flow over India was weak (approximately 10 kt). The period 22–31 July was characterized by a gradual reestablishment of the monsoon. Low-level westerlies strengthened over the

Arabian Sea and southern India while a depression formed over the Bay of Bengal (20°N, 92°E) on 27 July and moved inland on 28 July. The monsoon trough shifted southward of its mean position and was oriented approximately SE–NW at 20°N latitude. Convective activity increased during this period over both India and the Bay of Bengal. Fig. 3 shows the 29 July surface map indicative of active monsoon conditions.

3. Data and analysis

a. Aircraft data

During the summer phase of MONEX 79, the NCAR Electra aircraft flew ten sorties from the period 5–28 July 1979. The 14 July boundary layer mission considered here was designed to study vertical fluxes of energy and momentum in the boundary layer over the Bay of Bengal. Figure 4 shows the Electra flight track along with ship positions for 14 July. The research flight was made in a northeast–southwest direction roughly along the near-surface mean wind trajectory. Stepped low-level crosswind legs of approximately 8 min, each at the northern (profiles at approximately 19.9°N, 88.9°E) and southern (profiles at 16.2°N, 87.2°E) ends of the flight track, provide the aircraft
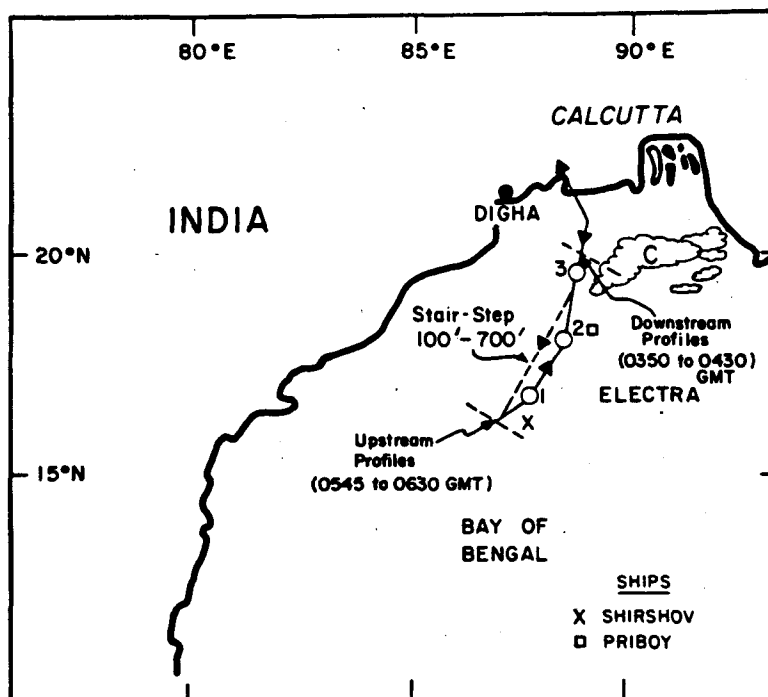

FIG. 4. Flight track of the NCAR Electra aircraft for 14 July 1979 over the Bay of Bengal. Open circles indicate dropwindsondes launched. Flight track was generally along mean surface wind. The main aircraft data base for this study was collected along the upstream and downstream profile regions. Ship positions are also given. The cloud region sketched near 19.7°N, 89.5°E and designated by C was obtained from satellite photographs.

data for this paper. Five boundary layer legs were flown over each region, with each leg approximately 30 km in length. Flight levels over the northern region were at altitudes 76, 164, 249, 406 and 663 m; those over the southern region were at 88, 174, 271, 428 and 685 m. Examination of satellite pictures showed convective cells centered at approximately 19.7°N, 89.5°E (indicated in Fig. 4 as C) and covering part of the northern region.

Reports from observers on board the Electra indicate extensive cloudiness throughout the observation region with the northern end of the flight track generally showing more towering cumulus and convective activity than the southern end. Cloud bases as low as 400 m were observed. Thus, due to the differences in cloud patterns between the northern and southern Bay of Bengal regions of the Electra flight track, results are presented separately for the two regions.

Details on the instrumentation of the NCAR Electra aircraft are given in the SMONEX Field Phase Report (WMO, 1981). The Electra gust probe system which measures the motion of the air relative to the aircraft was the principal instrumentation used for wind speed and direction observations. The Electra inertial navigation system (INS) located at the base of the 5.2 m nose boom on the center line measures the motion of the aircraft with respect to the ground and provided latitude and longitude, heading, ground speed and aircraft vertical velocity. Combining gust probe measurements and the inertial platform system allows for both mean and turbulent components to be resolved in terms of a coordinate system relative to the earth. A Lyman-alpha hygrometer provided fast-response (20 s^{-1}) values of humidity. Dropwindsondes from the Electra on 14 July were also used to study the mean boundary layer structure.

b. Digha observations

The boundary layer experiment at Digha (location shown in Fig. 4) consisted of three main components: 1) a 10 m micrometeorological tower at the beach with instruments to observe turbulent fluxes of heat and momentum over the ocean, 2) a weather station that continuously recorded mean parameters, and 3) pilot balloon observations to a height of about 1000 m.

Pilot balloon soundings were made to determine the wind speed and direction in the marine boundary layer over the Bay of Bengal. These soundings were made at 1000, 1400, 1700, 2100 and 0100 GMT each day except when haze, fog or cloud conditions prevented a launch. The ascent rate was about 100 m min^{-1} and the observations were made at intervals of 30 s during each sounding. Thus a greater resolution in the boundary layer not possible with conventional radiosonde soundings was available. Observations from the micrometeorological tower and pilot balloon soundings

were made at Digha from 14 July to 4 August 1979. A description of the observation system is given elsewhere (SethuRaman et al., 1980). Wind direction during the experiment was predominantly south-southwesterly and onshore greater than 95% of the observation period; data presented here are only for onshore flows. Steadiness, defined as the ratio of the vector averaged wind and the mean wind speed was calculated to be approximately 90% for the 100 to 500 m layer at Digha during the period 1700 GMT on 15 July to 2100 GMT on 18 July. Fetches over the ocean for 14 July at Digha, obtained by using backward trajectory analysis of mean wind speed and direction data every 12 h, were on the order of 500 to 700 km.

c. Ship data

Radiosondes launched from the Russian ships *Shirshov* and *Priboy* located in the MONEX observation area (Fig. 4) during the period 14–29 July were used to obtain profiles of mean wind, temperature and humidity. The ships were stationary during this time period.

d. Analysis

Low-level flight data from the Electra consisted of high frequency (20 samples s^{-1}) fluctuations of components of wind speed (u, v, w), ambient temperature (T), and specific humidity (q). Relative to the mean value at one level the wind component has an accuracy of 0.1 m s^{-1}. Relative accuracies are 0.03 K for T and 0.01 g kg^{-1} for q (Kuettner et al., 1979). No trends were observed in the time histories and no filtering was performed. Corresponding low frequency (1 s^{-1}) measurements from the Electra were used as a means of quality control. Data with spurious spikes were eliminated. The mean, standard deviation and range of each variable were also obtained using standard statistical procedures.

The problem of contamination of thermodynamic fluxes by clouds or rain was remedied through careful analysis of Lyman-alpha humidity data. Moisture fluxes obtained from Lyman-alpha data were first compared with those from slow response instruments. A comparison of variances of specific humidity data between these two types of instruments was made, but with due regard for the difference in frequency response. If the variances were markedly different, the Lyman-alpha data were not used. We feel confident that contamination by rain on 14 July did not occur based on observer's reports. The Lyman-alpha performed remarkably well on this research day based on our analysis of the time history and evaluation of statistical parameters such as mean, variance and range.

High frequency data (20 s^{-1}) were used in flux computations. It consisted of a cross-covariance analysis of two appropriate time series. The dissipation rate ϵ of the turbulent kinetic energy was estimated from the

inertial subrange of the longitudinal velocity spectra using a Kolmogorov constant of 0.67 (Lenschow et al., 1980). Scaling parameters such as u_*, the friction velocity, w_*, the convective velocity scale, θ_*, the convective temperature, and L, the Monin-Obukhov length were calculated from

$$u_* = [(\overline{u'w'})_0{}^2 + (\overline{v'w'})_0{}^2]^{1/4}, \tag{1}$$

$$w_* = \left[\frac{g}{T}h(\overline{w'T_v'})_0\right]^{1/3}, \tag{2}$$

$$\theta_* = \frac{(\overline{w'T_v'})_0}{w_*}, \tag{3}$$

$$L = -\frac{\bar{T}_v u_*^3}{kg(\overline{w'T_v'})_0}, \tag{4}$$

where h is the mixed layer depth estimated as the height of the lowest inversion base, T_v is the virtual temperature, k is von Karman's constant (0.4), and g is gravitational acceleration. Primes denote turbulent quantities and overbars indicate a mean value taken over the length of the flight leg. Surface fluxes were derived from the bulk aerodynamic technique. Table 1 gives values of the parameters sampled by the Electra on 14 July for the two regions of the Bay of Bengal.

Determination of the mixed layer depths h from virtual temperature profiles agrees with the ones obtained from the profile of specific humidity (Fig. 5). Values of q obtained from a Lyman-alpha hygrometer are roughly constant throughout the boundary layer with a sharp decrease observed above approximately $z = h$.

4. Results

a. Mean profiles

Figure 6 shows the mean virtual temperature and wind speed profiles for 14 July over the northern region of the Bay of Bengal based on radiosonde, dropsonde and aircraft data. The thermal structure is characterized by a mixed layer to about 400 m capped by a strong inversion. Jetlike flow was observed in the wind speed profile with the maximum of about 13 m s^{-1} at an altitude of about 500 m. Synoptic conditions corresponded to a break in the monsoon (Fig. 2). Observations of wind direction data generally indicate slight veering (ranging from approximately 230° to 270°) from the surface to 800 mb for the period 12–15 July. This agrees with synoptic conditions generally showing southwest flow near the surface changing to a more westerly flow above the boundary layer. Figure 7,
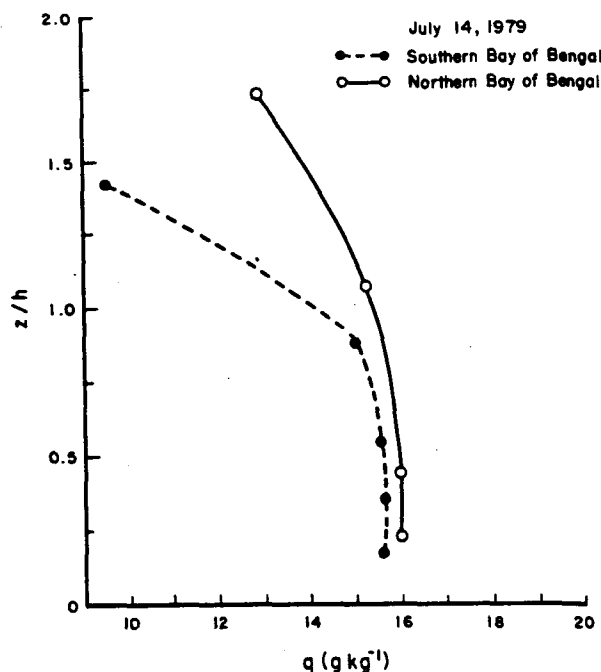

FIG. 5. Plot of vertical profile of specific humidity q over the southern and northern Bay of Bengal versus normalized height z/h.

showing u and v wind components for the northern and southern Bay of Bengal regions on 14 July obtained from the NCAR Electra, also supports this observation.

Aircraft observations in the boundary layer over the Bay of Bengal were only available for 14 July 1979. However, some of the interesting features of the boundary layer structure observed on this day were also evident from analyzed wind and temperature profiles obtained over the Bay of Bengal on other days using other platforms, such as ships. Virtual potential temperature profiles taken from the U.S.S.R. research vessel *Shirshov* at 16.2°N, 87.7°E at 0600 and 1800 GMT on 12 July 1979 are shown in Fig. 8. Break monsoon conditions also existed this day. The horizontal temperature gradient near the surface estimated from ship data was approximately 0.005°C km^{-1}. Temperature profiles obtained from radiosonde soundings do not have good resolution in the marine boundary layer, but general features of the thermal structure can be inferred. It is characterized by a slightly unstable layer near the surface and a mixed layer of 500 m capped by a strong stable layer and is essentially similar to the one on 14 July previously discussed. Wind profiles for

TABLE 1. Boundary layer parameters: 14 July 1979.

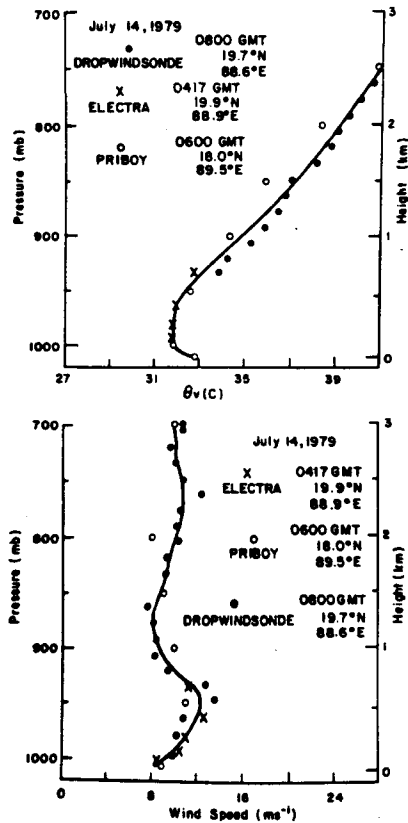| Region	h (m)	L (m)	w_* (m s^{-1})	u_* (m s^{-1})	θ_* (C)
Southern Bay of Bengal (16.2°N, 87.2°E)	500	−140	0.66	0.32	0.027
Northern Bay of Bengal (19.9°N, 88.9°E)	400	−255	0.57	0.36	0.025

FIG. 6. Vertical variation of mean virtual potential temperature θ_v and mean wind for 14 July 1979 obtained from ship, dropwindsonde and low-level NCAR Electra data.

the same time periods on 12 July show the existence of a low-level jet. Maximum wind speeds were observed at a height about 500 m, which is slightly higher than the base of the capping inversion. Thus it appears the height of the boundary layer over the Bay of Bengal was relatively shallow as compared to the Arabian Sea where the heights ranged from 800 to 1500 m (Holt and SethuRaman, 1985). Maximum winds at or slightly higher than the height of the boundary layer have also been observed by Long (1980) for the monsoon boundary layer. Augstein (1978) observed the wind speed maximum to lie in the upper part of the mixed layer in the trade regions with shallow mixed layers.

Radiosonde observations of virtual potential temperature from a U.S.S.R. ship (16.2°N, 87.7°E) are given in Fig. 9 for 22 July 1979 as an example of typical monsoon active conditions. Also given is a profile of θ_v observed at Digha by radiosonde sounding with onshore airflow. Except for the warming of the air, the profiles are essentially similar with a shallow mixed layer consisting of neutral to slightly stable air to about 500 m and a capping inversion aloft. The observed wind profiles indicate a lack of the low-level jet observed during monsoon-break conditions on 12 and 14 July (Figs. 8 and 6, respectively).

b. Balance of forces along mean trajectory

Computations of forces along a mean trajectory for 14 July 1979 over the Bay of Bengal were carried out in order to understand the balance of these forces in
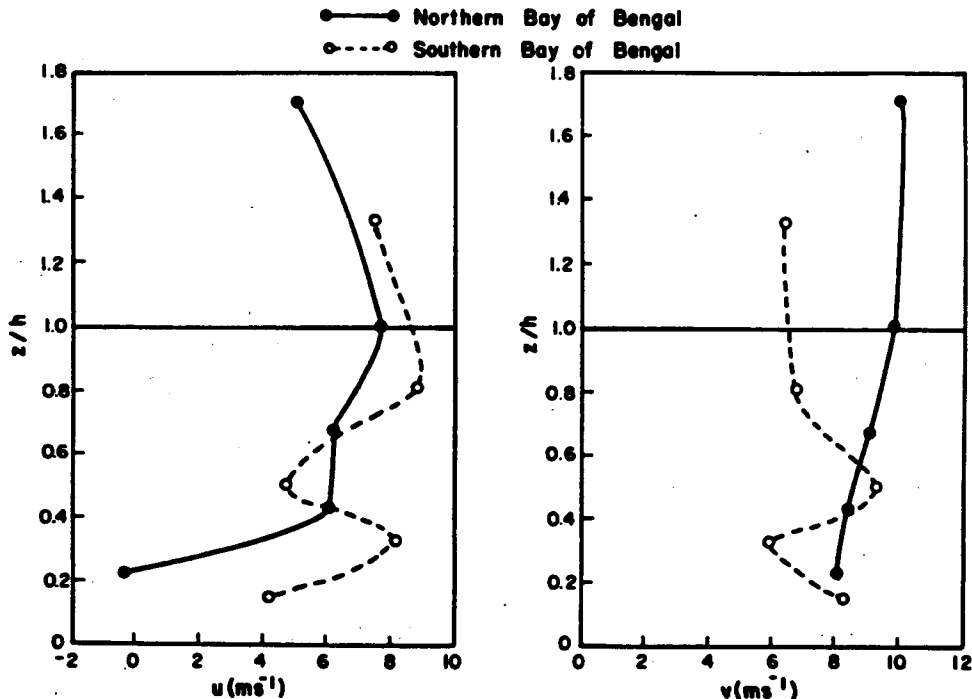

FIG. 7. Vertical profiles of u and v wind components for the northern and southern Bay of Bengal on 14 July 1979 obtained from NCAR Electra gust probe data.
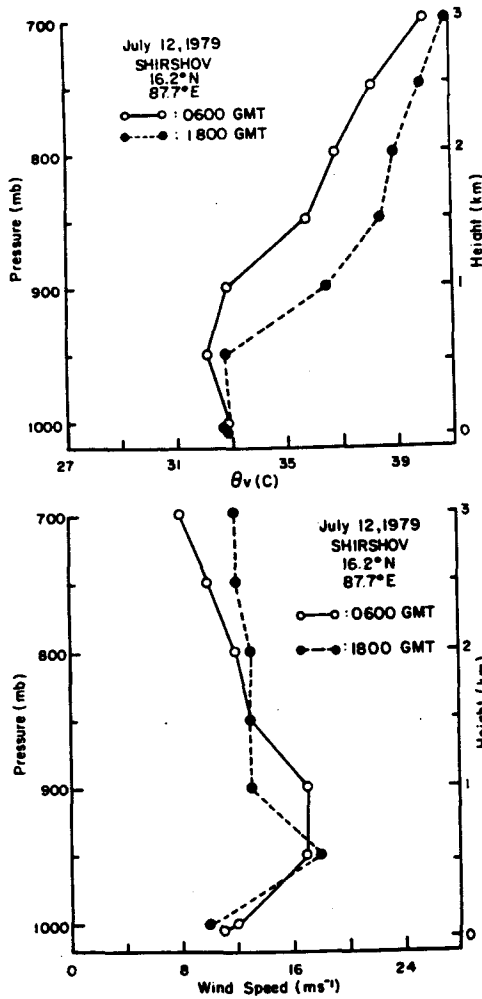
July 12, 1979
SHIRSHOV
16.2°N
87.7°E
o——o : 0600 GMT
●----● : 1800 GMT

July 12,1979
SHIRSHOV
16.2°N
87.7°E
o——o : 0600 GMT
●---● : 1800 GMT

FIG. 8. Vertical variation of mean virtual potential temperature θ_v and mean wind for 12 July 1979 obtained from the U.S.S.R. research ship *Shirshov*. Note the similarity to Fig. 6; both days were characterized by break conditions.

the monsoon boundary layer. For mean horizontal flow with homogeneous turbulence, the equations of motion may be written as

$$
\begin{aligned}
\frac{d\bar{V}_s}{dt} + f(\bar{V}_{gn} - \bar{V}_n) &= \frac{1}{\rho}\frac{\partial \bar{\tau}_s}{\partial z} \\
\frac{d\bar{V}_n}{dt} - f(\bar{V}_{gs} - \bar{V}_s) &= \frac{1}{\rho}\frac{\partial \bar{\tau}_n}{\partial z}
\end{aligned}
\right\} \quad (5)
$$

where "*s*" and "*n*" refer to components parallel and perpendicular, respectively, to the surface wind, $\tau = (\tau_s, \tau_n)$ represents the wind stress, $V_g = (V_{gs}, V_{gn})$ represents the geostrophic wind, and overbars denote ensemble averages.

The flight track of the NCAR Electra research aircraft (Fig. 4) for 14 July was approximately along the mean surface trajectory within ±10 deg. Lateral and longitudinal gusts measured by the NCAR Electra aircraft can thus be used as an approximation to the tangential

and normal components "*s*" and "*n*," although the lateral wind is somewhat more sensitive to deviations from zero drift. The mean longitudinal wind, $\bar{V}_s$, and the mean lateral wind, $\bar{V}_n$, were obtained from averages over each run. Dropwindsonde data over the region of the flight tracks give mean surface data at approximately 990 mb.

The Lagrangian acceleration term $d\bar{V}_s/dt$ along a streamline with the *s* direction positive downstream and the *n* direction positive to the right can be approximated from

$$
\frac{d\bar{V}_s}{dt} = \frac{\partial \bar{V}_s}{\partial t} + \bar{V}_s \frac{\partial \bar{V}_s}{\partial s} + \bar{w}\frac{\partial \bar{V}_s}{\partial z} \quad (6)
$$

where $\bar{w}$ is the mean vertical velocity and partial derivatives $\partial/\partial t$, $\partial/\partial s$ and $\partial/\partial z$ represent local change,
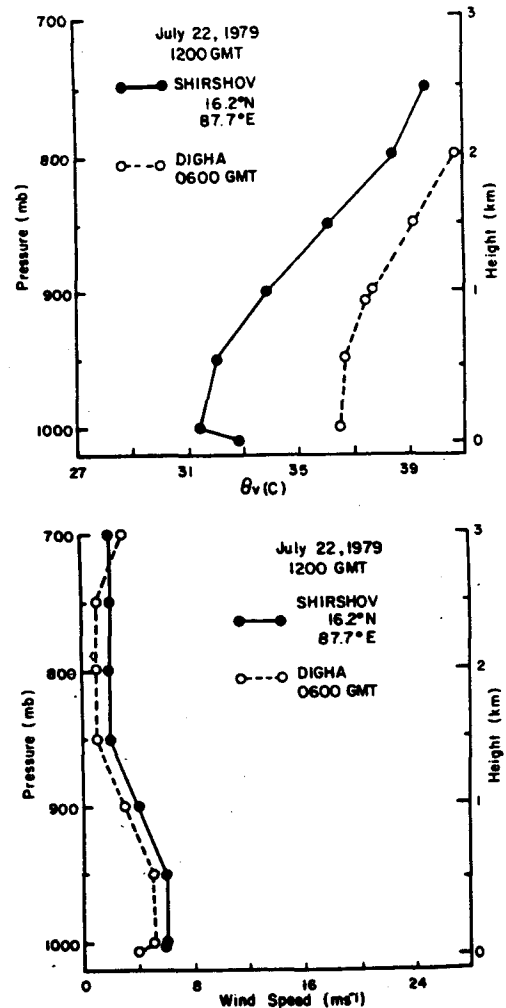

July 22, 1979
1200 GMT
●——● SHIRSHOV
16.2°N
87.7°E
o---o DIGHA
0600 GMT

July 22, 1979
1200 GMT
●——● SHIRSHOV
16.2°N
87.7°E
o---o DIGHA
0600 GMT

FIG. 9. Vertical variation of mean virtual potential temperature θ_v and mean wind speed for 22 July 1979 from the coastal site at Digha (dashed line) and the U.S.S.R. ship *Shirshov* (solid line). Onshore flow existed this day with a warming of approximately 5°C between Digha and the ship. Both temperature profiles indicate a neutral to slightly stable layer to approximately 500 m capped by a strong inversion. Note the lack of low-level jet in the wind profile.

variation along streamline and vertical advection, respectively. Effect of the curvature of streamlines is neglected. Analysis of wind speed and direction data at 1000 mb (approximately 90 m above the ocean) obtained from the stationary U.S.S.R. ships *Shirshov* (16.2°N, 87.7°E) and *Priboy* (18.0°N, 89.5°E) for the period 0000 GMT 11 July to 1800 GMT 15 July yield a mean wind speed value of 9.1 m s^{-1} and mean wind direction of 230°. Standard deviations are 1.6 m s^{-1} and 10° for the wind speed and direction, respectively. Thus, assuming quasi-stationarity ($\partial V_s/\partial t \approx 0$) and no cross-stream gradient ($\partial/\partial n = 0$), the mean vertical velocity $\bar{w}$ can be approximated from the two-dimensional divergence equation integrated over a depth z as

$$\bar{w} = \int_0^z \text{div} V dz \sim \frac{\Delta V_s}{\Delta s} z \qquad (7)$$

where $\text{div}V \approx \Delta V_s/\Delta s$.

Components of the geostrophic wind, lateral component V_{gn} and longitudinal component V_{gs} were calculated from both dropwindsonde data and an analysis of geostationary satellite data at about 900 mb (Stout and Young, 1983), with the 900 mb wind assumed to be geostrophic. A simple finite difference scheme was used to estimate the geostrophic components V_{gn} and V_{gs} at 900 mb from dropwindsonde wind speed and direction data. Linear interpolation of values from Stout and Young's (1983) mean wind field for this day over the Bay of Bengal yielded similar results.

Values for the gradient of the wind stress $\bar{\tau}_s$ were approximated from the stress profiles and a centered finite difference scheme. The drag coefficient formulation given by Large and Pond (1981) is

$$\tau = \rho(0.49 + 0.065 U_{10}) \times 10^{-3} U_{10}{}^2 \qquad (8)$$

where U_{10}, the wind speed in m s^{-1} at 10 m, is used to extend the stress term to the surface.

The plot of the vertical variation of the various forces for 14 July over the Bay of Bengal is given in Fig. 10. Values of the different forces were calculated at three altitudes from aircraft data: 90, 250 and 540 m. Values near the surface for the geostrophic departure and acceleration terms were estimated as extensions of the observations and are denoted by dotted lines. The results are comparable to those over the Arabian Sea (Holt and SethuRaman, 1985). The overall balance is generally between the acceleration term (order of 10^{-3} m s^{-2} near the surface) and friction term (10^{-3} m s^{-2}) with geostrophic departure an order of magnitude smaller (10^{-4} m s^{-2}). As compared to trade wind boundary layers (Brümmer, 1976; Holland and Rasmusson, 1973), the balance of forces in the monsoon boundary layer is markedly different. Acceleration is a major source term in the monsoon boundary layer but can generally be neglected in trade wind boundary layers (Augstein, 1978). Acceleration and friction approximately balance in the monsoon boundary layer
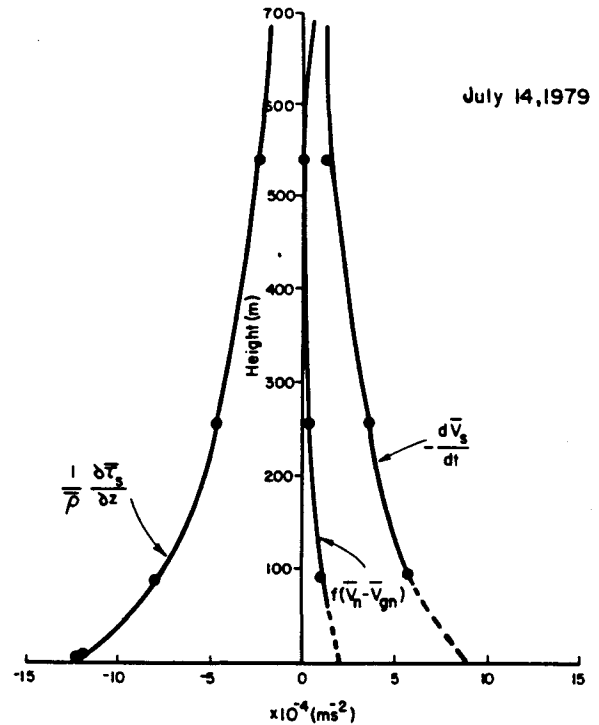

FIG. 10. Balance of forces for 14 July 1979 over the Bay of Bengal showing the vertical variation of geostrophic departure [$f(\bar{V}_n - \bar{V}_{gn})$], advective acceleration ($d\bar{V}_s/dt$) and friction ($1/\rho)(\partial\bar{\tau}_s/\partial z$). Solid circles show values obtained from aircraft data. Lines were drawn as eye averages.

over the Bay of Bengal while friction and geostrophic departure are the dominant terms in trade wind regions. A summary of the orders of magnitudes for various terms for monsoon and trade wind boundary layers (Augstein, 1978) is given in Table 2.

As seen in Table 2 there is an imbalance, roughly 5 × 10^{-5} m s^{-2}, in the comparison of forces along a trajectory for the three levels studied over the Bay of Bengal. In the typical trade wind boundary layer (Augstein, 1978) forces roughly balance. Assumptions of constant geostrophic wind with height in the monsoon boundary layer along with no cross-stream gradients could contribute to the imbalance. An analysis of turbulent quantities of temperature, humidity and wind components presented in subsection 4d also indicates that the assumption of homogeneous turbulence could be a contributing factor to the imbalance. Scatter in the curves is also a source of error.

c. Flux profiles

Figure 11 shows the turbulent flux profiles of virtual temperature $\overline{w'T_v'}$, temperature $\overline{w'T'}$ and specific humidity $\overline{w'q'}$ for the southern and northern Bay of Bengal on 14 July 1979. Virtual temperature flux was calculated from the relationship:

$$\overline{w'T_v'} = \overline{w'T'} + 0.61 \, \bar{T}\overline{w'q'}. \qquad (9)$$

TABLE 2. Comparison of the forces (m s^{-2}) along a trajectory for trade wind and monsoon boundary layers near the ocean surface.

Level (m)	Friction ($\times 10^{-5}$)	Geostrophic departure ($\times 10^{-5}$)	Advective acceleration ($\times 10^{-5}$)
	Trade Wind (typical)		
90	14	12	2
250	10	9	1
540	6	6	1
	Monsoon (Bay of Bengal)		
90	80	20	60
250	50	10	45
540	25	1	20

The profiles are similar for both regions. It is interesting to note that sensible heat flux $\overline{w'T'}$ changes sign at a low altitude, approximately $z = 0.45\ h$ (about 200 m). Nicholls and LeMone (1980) also observed this for undisturbed conditions over the tropical ocean using GATE data.

The profiles of virtual heat flux $\overline{w'T_v}$ are essentially unchanged for both the northern and southern regions independent of cloud amount. Figure 12 shows the virtual heat flux for both regions normalized by the surface value $(\overline{w'T_v})_0$. The dotted line is drawn by eye and is constrained to go through $\overline{w'T_v} = (\overline{w'T_v})_0$ at the surface. A linear fit used in many simple mixed layer models does not appear applicable here. A value of

-0.28 for $\overline{w'T_v}/(\overline{w'T_v})_0$ at roughly $z = h$ is comparable to the value -0.21 obtained by Betts (1976) from cumulus convection over land and -0.20 in numerical simulations by Sommeria (1976) and Sommeria and LeMone (1978), but the data for the Bay of Bengal presented here are somewhat skewed toward zero in the lowest half of the boundary layer—as opposed to larger values given by a linear fit. Thus the decreased effect of vertical flux appears important for this case over the Bay of Bengal boundary layer.

Figure 13 shows the momentum fluxes $\overline{u'w'}$ and $\overline{v'w'}$ for the two regions on 14 July 1979. Each profile is similar, in that values are negative up to approximately $z = 0.3$ to $0.45\ h$, with values near the top of the boundary layer about 0.04 to 0.08 m^2 s^{-2}. Surface values obtained from bulk methods [see Eq. (8)] range from approximately -0.02 to -0.13 m^2 s^{-2}. Profiles of momentum fluxes $\overline{u'w'}$ and $\overline{v'w'}$ normalized by surface values $(\overline{u'w'})_0$ and $(\overline{v'w'})_0$, respectively (not shown here), indicate large values near the top of the boundary layer. Normally, one would expect the momentum fluxes to decrease monotonically with height, approaching zero at $z = h$. It appears the suppressed convection over the Bay of Bengal and the associated jet could be a cause of the large positive stress. Another possible reason could be the organized cloud motions. Unfortunately, the only specific cloud data available during this study were obtained from limited satellite pictures and reports from observers onboard the Electra. Thus, influences of clouds on fluxes and turbulence
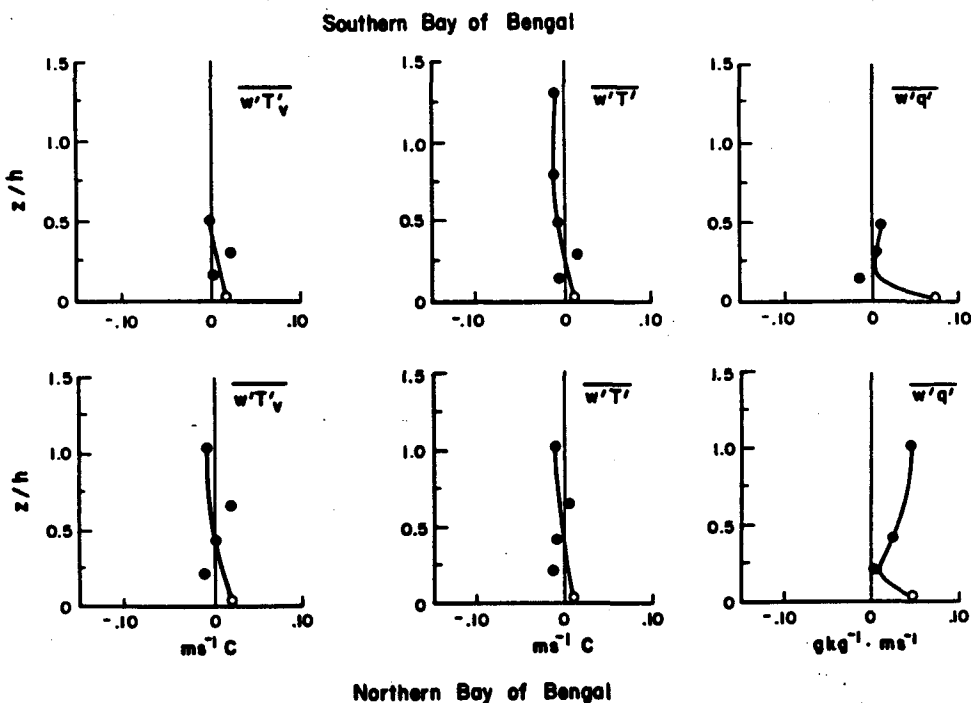
Southern Bay of Bengal

Northern Bay of Bengal

FIG. 11. Profiles of virtual temperature flux $\overline{w'T_v}$, temperature flux $\overline{w'T'}$ and specific humidity flux $\overline{w'q'}$ on 14 July 1979 for the southern and northern Bay of Bengal.
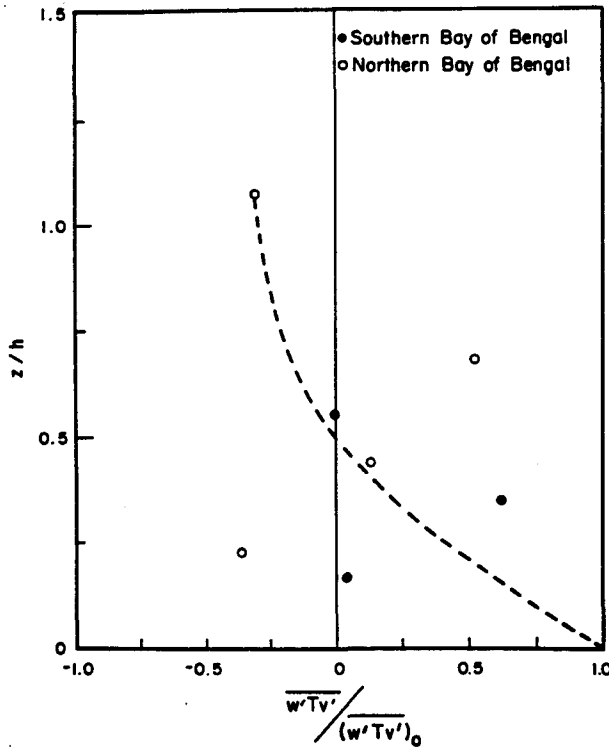
FIG. 12. Profile of virtual temperature flux $\overline{w'T_v'}$ normalized by the surface value for both southern and northern Bay of Bengal.

are not well substantiated for this time period over the Bay of Bengal.

d. Turbulence profiles

Figure 14 shows the vertical structure of the dimensionless standard deviations of velocity components observed over the Bay of Bengal. Also included are Willis and Deardorff's (1974) curve obtained from water tank simulation of cloud-free convection and the free convection curve based on Kansas data (Wyngaard et al., 1971). Values of w_* along with other parameters for the two regions over the Bay of Bengal are given in Table 1.

Maximum values of σ_w/w_* occur roughly at a height of $z = 0.6\ h$. Others (Nicholls and LeMone, 1980; Kaimal et al., 1976) have found maximum values to occur at about $z = 0.5\ h$. Values over the northern region are generally larger than those over the southern region, as was expected due to increased convection. As also noted by Nicholls and LeMone (1980) in their comparison of clear and partly cloudy conditions, higher ratios of σ_w to w_* are observed near cloud base over the Bay of Bengal.

Because u and v turbulence did not differ significantly over each flight leg of the two regions, the average of the standard deviations of east–west and north–south wind speed, $\sigma_{u,v}$, normalized by w_* is presented here in Fig. 14. The lateral and longitudinal turbulence is

slightly greater in the monsoon boundary layer over the Bay of Bengal than can be simulated in the laboratory. Obviously, the presence of the low-level jet over the Bay of Bengal during monsoon break conditions is important in generating lateral and longitudinal turbulence. Using surface layer data, Panofsky et al. (1977) approximated $\sigma_{u,v}$ by

$$\sigma_{u,v} = u_*(12 + h/|L|)^{1/3}. \qquad (10)$$

Values of $\sigma_{u,v}$ of 0.91 and 1.12 m s^{-1} were obtained over the southern and northern regions, respectively, using this formulation. This agrees better with observed values.

The normalized temperature variance σ_T^2/θ_*^2 is shown in Fig. 15 along with free convection and laboratory curves as in Fig. 14. Values up to a height of approximately $z = 0.5\ h$ agree roughly with the free convection prediction. However, the greatest deviation from both laboratory and free convection curves occurs above $z = 0.6\ h$. Numerical model results of Deardorff (1974) indicate that entrainment is directly associated with the large increases in temperature variance near the inversion base. However, entrainment appears to be significant at much lower levels in the monsoon boundary layer. Willis and Deardorff (1974) give a value of approximately $\sigma_T = 10\theta_*^2$ at the top of the boundary layer due primarily to entrainment. Over the northern and southern Bay of Bengal regions, values of this magnitude are found at levels as low as $z = 0.4\ h$.

e. Turbulent kinetic energy budget

The turbulent kinetic energy budget in the boundary layer, under the assumption of negligible horizontal advection of kinetic energy $\bar{u}(\partial\bar{e'}/\partial x)$, is given by

$$\frac{\partial\bar{e'}}{\partial t} = \frac{g}{T_v}\overline{w'T_v'} - \frac{\tau}{\rho}\cdot\frac{\partial V}{\partial z} - \frac{\partial}{\partial z}\left[\overline{w'e'} + \frac{\overline{w'p'}}{\rho}\right] - \epsilon \qquad (11)$$

where $\bar{e'}$ is the kinetic energy equal to $\frac{1}{2}(\overline{u'^2} + \overline{v'^2} + \overline{w'^2})$, τ the stress, ρ the density, $\partial V/\partial z$ the vertical shear, and ϵ the energy dissipation rate. The time rate of change of kinetic energy $\partial\bar{e'}/\partial t$ was on the order of 10^{-5} m^2 s^{-3} for 14 July 1979, approximately two orders of magnitude smaller than the other terms, and was assumed negligible over the Bay of Bengal for this day. Horizontal advection of kinetic energy, $\bar{u}(\partial\bar{e'}/\partial x)$, was approximated by finite difference also to be on the order of 10^{-5} m^2 s^{-3}. Thus, Eq. 11 can be rewritten as

$$\frac{g}{T_v}\overline{w'T_v'} - \left(\overline{u'w'}\frac{d\bar{u}}{dz} + \overline{v'w'}\frac{d\bar{v}}{dz}\right)$$

$$- \frac{\partial}{\partial z}\left(\overline{w'e'} + \frac{\overline{w'p'}}{\rho}\right) - \epsilon = 0. \qquad (12)$$

Figures 16 and 17 show the turbulent kinetic energy budget for 14 July 1979 over the southern (approximate
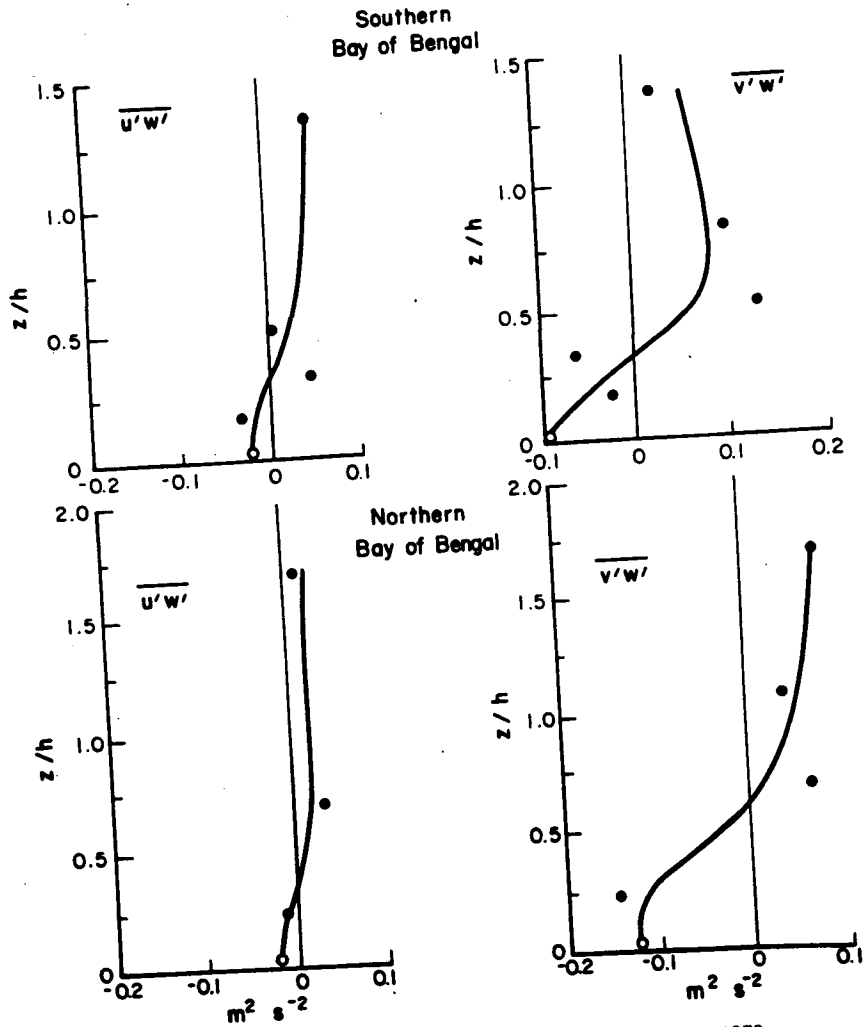
FIG. 13. Profiles of momentum fluxes $\overline{u'w'}$ and $\overline{v'w'}$ on 14 July 1979 for the southern and northern Bay of Bengal.

location 16.2°N, 87.2°E) and northern Bay of Bengal (19.9°N, 88.9°E), respectively, with all terms normalized by the surface heat flux $(g/T_v)(\overline{w'T'_v})_0$. Surface values were obtained using the bulk aerodynamic method. Solid curves were drawn by eye through the computed values of buoyancy $(g/T_v)\overline{w'T'_v}$, shear $[-\overline{u'w'}(d\bar{u}/dz) - \overline{v'w'}(d\bar{v}/dz)]$, dissipation ϵ and vertical turbulent transport $(\partial/\partial z)(\overline{w'e'})$. Vertical gradients were calculated by a centered finite difference scheme with flux values obtained from aircraft data during each particular leg. The pressure transport term $(\partial/\partial z)(\overline{w'p'})$ was not calculated and was estimated as a residual. The fact that the buoyancy term is fairly insensitive to changes in convection conditions (as mentioned before) results in similar buoyancy profiles over the two regions. For both the southern $(L \simeq -140 \text{ m})$ and northern Bay of Bengal $(L \simeq -255 \text{ m})$, buoyancy is the primary source of kinetic energy near the surface up to

approximately $z = 0.15\ h$. However, shear becomes the dominant source term above $z = 0.15\ h$ up to about $z = 0.7\ h$. Over the northern Bay of Bengal up to about $z = 0.75\ h$, vertical turbulent transport and dissipation are the primary sinks of kinetic energy while over the southern region dissipation is a more dominant sink term than vertical turbulent transport. Above approximately $z = 0.75\ h$, heat flux becomes negative over both regions, indicating the increased importance of the clouds.

Shear approaches zero near the top of the boundary layer over the northern Bay of Bengal (Fig. 17) but appears to have a finite value above $z = h$ over the southern region (Fig. 16). In the upper part of the boundary layer, transport is the dominant source term balancing dissipation. Sommeria and LeMone (1978) presented results from the NCAR 1972 Puerto Rico experiment in the fair weather mixed layer over the

tropical ocean and found a similar balance in the upper boundary layer. Results from a marine convective boundary layer during AMTEX presented by Lenschow et al. (1980) also agree qualitatively with the results presented here. However, their balance in the lower levels indicates buoyancy production as an important source term to a height of approximately $z = 0.8\ h$ as opposed to a height of $z = 0.6\ h$ in the monsoon boundary layer.

Using Lenschow's (1974) model of the turbulent kinetic energy budget with aircraft data from the Electra on 14 July as an input, values for buoyancy, shear and dissipation throughout the boundary layer were calculated. Although Lenschow's model development was based on over-land convective conditions, it would be of interest to compare the present results with the model. Lenschow specified that measurements of heat flux over land indicate the flux is zero somewhere between $z/h = 0.85$ and 0.90 and hence assumed that at $z/h = 0.87$, $B = 0$. Thus, for the two regions over the Bay of Bengal for 14 July, Lenschow's buoyancy flux equation can be written as

$$B = 1 - 1.15\,z/h, \quad 0 < z/h < 0.87. \qquad (13)$$

The shear (S) and dissipation (D) equations given by Lenschow are

$$S = -\frac{L}{h}\left\{\frac{[1 - 15(h/L)z/h]^{-1/4}}{z/h}\right\}, \qquad (14)$$

$$D = 0.43 + \left\{\frac{0.57}{\langle S\rangle + 3.75}[\langle S\rangle - S]\right\} + S, \qquad (15)$$

where

$$\langle S\rangle = -\frac{L}{h}\left\{\ln\frac{h}{z_0} - \left[2\ln\left(\frac{1+x}{2}\right)\right.\right.$$
$$\left.\left. + \ln\left(\frac{1+x^2}{2}\right) - 2\tan^{-1}x + \frac{\pi}{2}\right]\right\},$$

$$x = \left[1 - 15\frac{h}{L}\right]^{1/4}.$$

Parameters for Lenschow's equations, L and h were given in Table 1 for the northern and southern Bay of Bengal. Roughness length z_0 was taken to be 0.001 m.

Transport as prescribed by Lenschow was calculated as a residual and includes both vertical transport and pressure transport. Wyngaard and Coté (1971), McBean and Elliott (1975), Rayment and Caughey (1977) and Caughey and Wyngaard (1979) all suggested that pressure transport could be a significant term in the surface layer. For the two regions presented here, pressure transport appears as an important source term up to approximately $z = 0.6\ h$. Sommeria and LeMone (1978) show pressure transport to be an important source term up to about $z = 0.25\ h$.

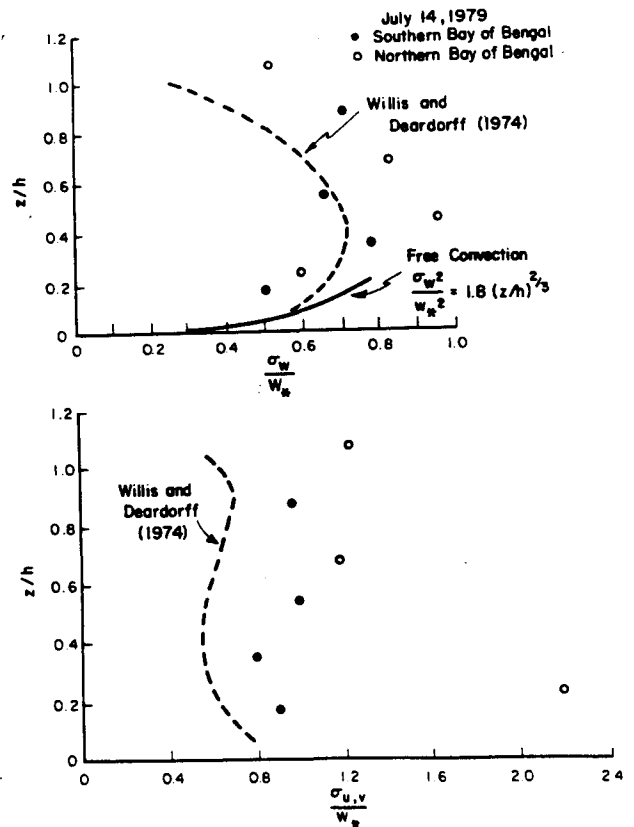In general, Lenschow's model tends to overestimate

FIG. 14. Profile of standard deviation of vertical velocity σ_w normalized by w_* along with the average of standard deviation of u and v velocity components $\sigma_{u,v}$ normalized by w_* for both the southern and northern Bay of Bengal. The solid line is the free convection line calculated from $\sigma_w/w_*^2 = 1.8(z/h)^{2/3}$ and the dashed line from Willis and Deardorff's (1974) laboratory experiments.

each term in the turbulent kinetic energy budget. In terms of dissipation, LeMone (1980) also observed overestimation using GATE data. Agreement is reasonable for the shear term but the linear relationship for buoyancy used in the model does not appear to hold for the monsoon boundary layer. The incorporation of L, h and the use of virtual temperature in Lenschow's model derived for use over land apparently is not sufficient to effectively model the large decrease in the buoyancy production in the lowest hundreds of meters in the monsoon boundary layer over the Bay of Bengal. Entrainment in the monsoon boundary layer appears to be an important process. Also, the effects of clouds in the boundary layer need more investigation.

5. Conclusions

Observations of mean wind profiles over the Bay of Bengal during MONEX 79 show a jet or wind maximum in the upper layers of the boundary layer during breaks in the monsoon when the monsoon trough migrates north to the foothills of the Himalayas. Wind
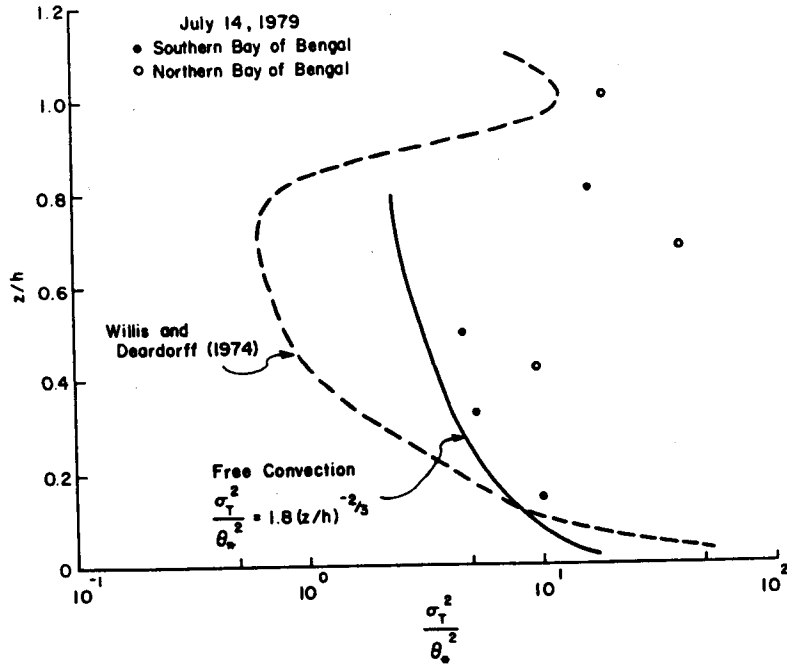
FIG. 15. Profile of temperature variance σ_t^2 normalized by θ_*^2 for the southern and northern Bay of Bengal on 14 July 1979. Solid line is the free convection prediction given by $\sigma_T^2/\theta_*^2 = 1.8(z/h)^{-2/3}$. Dashed line is from Willis and Deardorff (1974) as in Fig. 14.

profiles obtained during active monsoon periods do not show this wind maximum. The thermal structure through the boundary layer during break periods shows near-neutral to slightly unstable stratification as opposed to slightly stable during active monsoon periods.

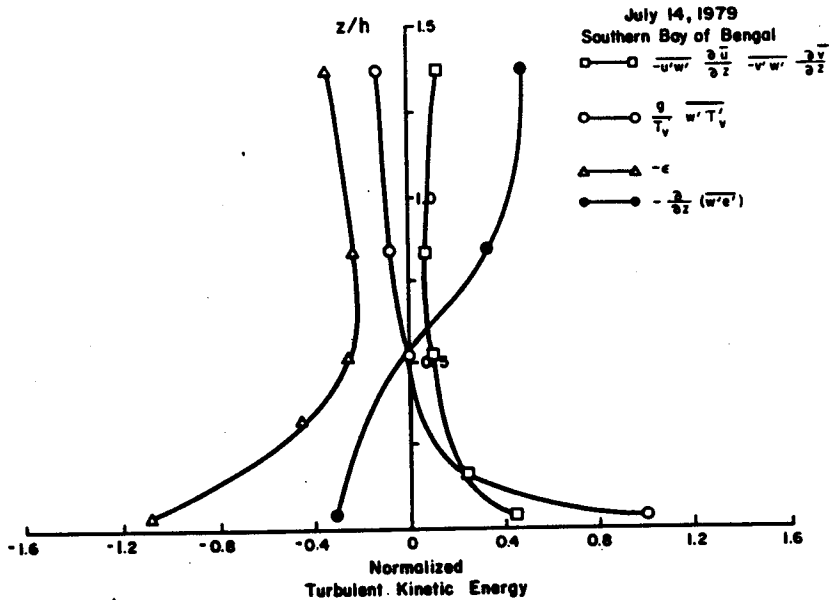Height of the boundary layer, as determined by the

FIG. 16. Profile of turbulent kinetic energy budget normalized by surface heat flux for 14 July 1979 over the southern Bay of Bengal. Aircraft observations are denoted on curve as shear, $\overline{-u'w'}\, \partial\bar{u}/\partial z - \overline{v'w'}\, \partial\bar{v}/\partial z$, (squares); buoyancy, $g/T_v\, \overline{w'T_v'}$, (open circles); dissipation, ϵ, (triangles); and vertical turbulent transport, $\partial/\partial z\, (\overline{w'e'})$, (solid circles).
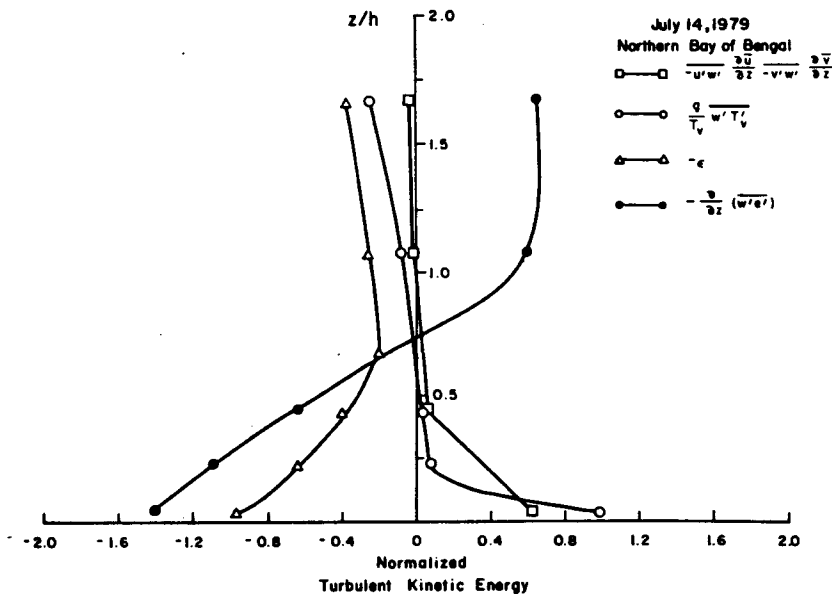
FIG. 17. As in Fig. 16 except for the northern Bay of Bengal.

height of the lowest inversion base, over the Bay of Bengal during active and break monsoons was observed to be about 400 to 500 m in contrast to about 800 to 1500 m reported for the Arabian Sea (Holt and SethuRaman, 1985).

There was an approximate balance of forces in the monsoon boundary layer over the Bay of Bengal between advective acceleration, geostrophic departure and friction. Geostrophic departure seems to play an important role in the balance only in the lowest 200 m. This agrees with results for the monsoon boundary layer over the Arabian Sea (Holt and SethuRaman, 1985). Advective acceleration in the monsoon boundary layer appears to be a significant term. In the trade wind regions, advective acceleration is generally negligible throughout the boundary layer. In the monsoon boundary layer, friction is approximately one order of magnitude larger than that over tropical oceans, while geostrophic departure is approximately the same order of magnitude for both monsoon and tropical boundary layers.

Observations of the turbulence structure obtained by the Electra also illustrate major differences between fair weather tropical and trade wind boundary layers and the monsoon boundary layer. Turbulent flux profiles seem to indicate the increased importance of entrainment in the monsoon boundary layer. Negative values of virtual heat flux occur at much lower altitudes over the Bay of Bengal and could be influenced by the large amount of clouds. Stronger moisture lapse rates and shear in the subcloud layer over the Bay of Bengal versus tropical or trade wind boundary layers also appear to be important.

Generally, turbulence values observed in the mon-

soon marine boundary layer are larger than those in tropical or trade wind boundary layers recorded in the literature. The presence of a low-level jet over the Bay of Bengal appears to have a strong influence.

The turbulent kinetic energy budget over the Bay of Bengal for 14 July (monsoon-break conditions) appears to show that the buoyancy is not the dominant source term throughout the depth of the monsoon boundary layer. However, it is an important source near the surface. There is a large gradient of both shear and buoyancy production in the lowest 30% of the monsoon boundary layer. Attempts at using Lenschow's (1974) model for an unstably stratified barotropic planetary boundary layer over land to estimate each term of the monsoon boundary layer turbulent kinetic energy budget gave reasonable profiles but generally overestimated the values.

Additional research and further coordinated observations are needed to understand possible interactions of the monsoon boundary layer with large-scale processes and its effect on the formation of depressions.

REFERENCES

Augstein, E., 1978: The atmospheric boundary layer over the tropical oceans. *Meteorology over Tropical Oceans*, D. B. Shaw, Ed., *Royal Meteor. Soc.*, 105–132.

Betts, A. K., 1976: Modeling subcloud layer structure and interaction with a shallow cumulus layer. *J. Atmos. Sci.*, 33, 2363–2382.

Brümmer, B., 1976: The kinematics, dynamics and kinetic energy budget of the trade wind flow over the Atlantic Ocean. *"Meteor." Forschungsergeb.*, B11, 1–24.

Caughey, S. J., and J. C. Wyngaard, 1979: The turbulence kinetic energy budget in convective conditions. *Quart. J. Roy. Meteor. Soc.*, 105, 231–239.

Deardorff, J. W., 1974: Three-dimensional numerical study of turbulence in an entraining mixed layer. *Bound.-Layer Meteor.*, 7, 199–226.

Donelan, M., and M. Miyake, 1973: Spectra and fluxes in the boundary layer of the trade wind zone. *J. Atmos. Sci.*, 30, 444–464.

Holland, J. Z., and E. M. Rasmusson, 1973: Measurements of the atmospheric mass, energy and momentum budgets over a 500 km square of the tropical ocean. *Mon. Wea. Rev.*, 101, 44–55.

Holt, T., and S. SethuRaman, 1985: Aircraft and ship observations of the mean structure of the marine boundary layer over the Arabian Sea during MONEX 79. *Bound.-Layer Meteor.*, 33, 259–282.

Kaimal, J. C., J. C. Wyngaard, D. A., Haugen, O. R. Coté, Y. Izumi, S. J. Caughey and C. J. Readings, 1976: Turbulence structure in the convective boundary layer. *J. Atmos. Sci.*, 33, 2152–2169.

Kotteswaram, P., and C. A. George, 1958: On the formation of the monsoon depressions in the Bay of Bengal. *Indian J. Meteor. Hydrol. Geophys.*, 9, 9–22.

Krishnamurti, T. N., and H. N. Bhalme, 1976: Oscillations of a monsoon system. Part I. Observational aspects. *J. Atmos. Sci.*, 33, 1937–1954.

——, R. Godbke, C. B. Chang, F. Carr and J. Chow, 1975: Study of a monsoon depression (I) Synoptic structure. *J. Meteor. Soc. Japan*, 53, 227–240.

Kuettner, J. P., W. C. Bolhofer and M. S. Unninayer, 1979: Summer MONEX Final Implementation Plan. U.S. MONEX Project Office/NCAR-7511-79-1, 155 pp. [Available from NCAR, Boulder, CO 80307.]

Large, W. G., and S. Pond, 1981: Open ocean momentum flux measurements in moderate to strong winds. *J. Phys. Oceanogr.*, 11, 324–336.

LeMone, M. A., 1980: The marine boundary layer. *Workshop on the Planetary Boundary Layer*, Boulder, Amer. Meteor. Soc., 182–246.

Lenschow, D. H., 1974: Model of the height variation of the turbulence kinetic energy budget in the unstable planetary boundary layer. *J. Atmos. Sci.*, 31, 465–474.

——, J. C. Wyngaard and W. T. Pennell, 1980: Mean-field and second-moment budgets in a baroclinic, convective boundary layer. *J. Atmos. Sci.*, 32, 1313–1326.

Long, C. S., 1980: Analysis of aircraft measurements of boundary layer turbulence in monsoonal flow. M.S. thesis, Dept. of Meteorology, University of Wisconsin–Madison, 93 pp.

McBean, G. A., and H. A. Elliott, 1975: The vertical transports of kinetic energy by turbulence and pressure in the boundary layer. *J. Atmos. Sci.*, 37, 753–766.

Nicholls, S., and M. A. LeMone, 1980: The fair weather boundary layer in GATE: The relationship of subcloud fluxes and structure to the distribution and enhancement of cumulus clouds. *J. Atmos. Sci.*, 37, 2051–2067.

Panofsky, H. A., H. Tennekes, D. H. Lenschow and J. C. Wyngaard, 1977: The characteristics of turbulent velocity components in the surface layer under convective conditions. *Bound.-Layer Meteor.*, 11, 355–361.

Pennell, W. T., and M. A. LeMone, 1974: An experimental study of turbulence structure in the fair-weather boundary layer. *J. Atmos. Sci.*, 31, 1308–1323.

Rao, Y. P., 1976: *Southwest Monsoon. Meteor. Monogr.*, No. 1/1976, India Meteor. Dept., 367 pp.

Rayment, R., and S. J. Caughey, 1977: An investigation of the turbulence balance equations in the atmospheric boundary layer. *Bound.-Layer Meteor.*, 11, 15–26.

SethuRaman, S., P. A. Michael, W. A. Tuthill and J. McNeil, 1980: An observation system used to study the marine boundary layer over Bay of Bengal during Summer MONEX 79. *Bull. Amer. Meteor. Soc.*, 61, 1204–1211.

Sikka, D. R., 1978: Some aspects of life history, structure, and movement of monsoon depressions. *Monsoon Dynamics*, T. N. Krishnamurti, Ed., Birkhauser Verlag, 1501–1529.

Sommeria, G., 1976: Three-dimensional simulation of turbulent processes in an undisturbed trade wind boundary layer. *J. Atmos. Sci.*, 33, 216–241.

——, and M. A. LeMone, 1978: Direct testing of a three-dimensional model of the planetary boundary layer against experimental data. *J. Atmos. Sci.*, 35, 25–39.

Stout, J. E., and J. A. Young, 1983: Low-level monsoon dynamics derived from satellite winds. *Mon. Wea. Rev.*, 111, 774–798.

Willis, G. E., and J. W. Deardorff, 1974: A laboratory model of the unstable planetary boundary layer. *J. Atmos. Sci.*, 31, 1297–1307.

WMO, 1981: The Summer MONEX field phase report. FGGE Operations Rep., Vol. 8, WMO, 344 pp.

Wyngaard, J. C., and O. R. Coté, 1971: The budgets of turbulent kinetic energy and temperature variance in the atmospheric surface layer. *J. Atmos. Sci.*, 28, 190–201.

——, —— and Y. Izumi, 1971: Local free convection, similarity, and the budgets of shear stress and heat flux. *J. Atmos. Sci.*, 28, 1171–1182.